



# Structural and Dielectric Properties of $\text{Pb}[(\text{Zr},\text{Sn})\text{Ti}]\text{NbO}_3$ Thin Films Deposited by Radio Frequency Magnetron Sputtering

Woo-Chang Choi<sup>†</sup>

Research Institute, Daeyang Electric Co., Ltd., Busan 604-030, Korea

Received April 14, 2010; Revised May 17, 2010; Accepted July 12, 2010

$\text{Pb}_{0.99}[(\text{Zr}_{0.6}\text{Sn}_{0.4})_{0.9}\text{Ti}_{0.1}]_{0.98}\text{Nb}_{0.02}\text{O}_3$  (PNZST) thin films were deposited by radio frequency magnetron sputtering on a  $(\text{La}_{0.5}\text{Sr}_{0.5})\text{CoO}_3$  (LSCO)/Pt/Ti/SiO<sub>2</sub>/Si substrate using a PNZST target with an excess PbO of 10 mole%. The thin films deposited at the substrate temperature of 500°C crystallized to a perovskite phase after rapid thermal annealing (RTA). The thin films, which annealed at 650°C for 10 seconds in air, exhibited good crystal structures and ferroelectric properties. The remanent polarization and coercive field of the fabricated PNZST capacitor were approximately 20  $\mu\text{C}/\text{cm}^2$  and 50  $\text{kV}/\text{cm}$ , respectively. The reduction of the polarization after  $2.2 \times 10^9$  switching cycles was less than 10%.

**Keywords:** Ferroelectric, PZT, Doping, Sputtering, Rapid thermal annealing

## 1. INTRODUCTION

Over the last decade, ferroelectric thin films have been widely investigated for nonvolatile memory applications [1-12]. Among ferroelectric materials, lead-zirconate-titanate (PZT) has been considered to be the most promising candidate for memory applications [1-3]. However, serious limitations have been encountered, such as the loss of Pb, fatigue, and space charges between the ferroelectric thin film and the electrode [2,3]. To address these problems, various ferroelectric and electrode materials, such as bismuth-based ( $\text{SrBi}_2\text{Ta}_2\text{O}_9$ ), barium-based ( $\text{BaTiO}_3$ ),  $\text{RuO}_2$ , and  $\text{La}_{0.5}\text{Sr}_{0.5}\text{CoO}_3$ , have been extensively studied [4-6]. But these materials exhibited low polarization and high resistivity. In contrast to the aforementioned ferroelectric materials, antiferroelectric materials exhibited 180° domain switching behavior. One hundred and eighty degree domain switching possesses better fatigue properties in comparison to 90° domain switching due to its smaller internal stresses [7,8]. Also, through a doping donor and appropriate electrode materials, antiferroelectric materials may encompass ferroelectric properties [8,9]. In this study, in order to improve the ferroelectric property and crystal-

linity of the antiferroelectric material, Sn and Nb were doped in PZT materials. The PNZST thin films were deposited on  $(\text{La}_{0.5}\text{Sr}_{0.5})\text{CoO}_3/\text{Pt}/\text{Ti}$  bottom electrode by a radio frequency (RF) magnetron sputtering method and were annealed by the rapid thermal annealing (RTA) method. The microstructural characteristics and electrical properties of the PNZST thin films were investigated under varying RF magnetron sputtering parameters and annealing conditions.

## 2. EXPERIMENTS

The substrates used in this experiment were (100)-oriented p-type Si wafers with a polished surface oxidized in a wet O<sub>2</sub> atmosphere. The thickness of the SiO<sub>2</sub> layer was approximately 600 nm. The LSCO/Pt/Ti electrode was prepared on SiO<sub>2</sub>/Si substrate by a RF magnetron sputtering method. The Pt (150 nm) thin films were used as a bottom electrode, and Ti (20 nm) thin films were used to increase adhesion. The LSCO thin films were deposited on Pt/Ti/SiO<sub>2</sub>/Si at 400°C and annealed at 700°C in O<sub>2</sub> ambient to serve as a tolerable barrier against Pb diffusion [10]. A LSCO target of 2 inch diameter was sputtered in an Ar and O<sub>2</sub> ambience with the gas pressure of 10 mtorr at the power of 50

<sup>†</sup> Author to whom all correspondence should be addressed:  
E-mail: future2014@nate.com

**Table 1.** Sputtering and annealing conditions of PNZST thin films.

Sputtering conditions	
Target	$Pb_{0.99}(Zr_{0.6}Sn_{0.4})_{0.9}Ti_{0.1}Nb_{0.02}O_3$ (10 mole% excess PbO)
RF power	80 W
Gas ratio	Ar : O <sub>2</sub> = 9 : 0.5
Base pressure	$1 \times 10^{-6}$ torr
Gas pressure	10 mtorr
Sub. temp.	350-550°C
Thickness	300 nm
Annealing conditions	
Atmosphere	air
Temperature	550-700°C
Time	5-60 seconds

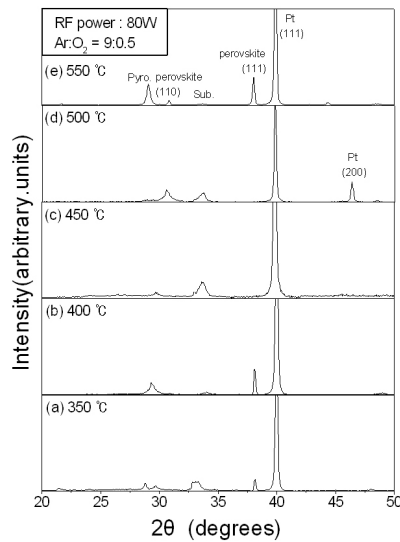


**Fig. 1.** X-ray diffraction patterns of PNZST thin films deposited at different substrate temperatures.

W. The thickness of the LSCO thin films was about 100 nm. Ferroelectric PNZST thin films were deposited at various conditions by a RF magnetron sputtering method. A PNZST target of 2 inch diameter was prepared by sintering at 1,150°C for 3 hours [10]. An excess of 10 mole% PbO powder was added to the target materials to compensate for the loss of Pb during deposition and post-annealing processes.

To improve crystallinity of the as-deposited PNZST thin films, the thin films were annealed at various conditions. The sputtering and annealing conditions of the thin films are summarized in Table 1. The Pt top electrodes with an area of 0.25 mm<sup>2</sup> were deposited by RF magnetron sputtering method and were defined by the lift-off process. The thickness of the thin films was measured by a surface profiler. The structural properties of the thin films were analyzed by X-ray diffraction using Cu-K<sub>α</sub> radiation. The measurements of electrical properties were carried out using an impedance analyzer and a ferroelectric tester.

### 3. RESULTS AND DISCUSSION

#### 3.1 Structural properties

The crystallinity of PZT-based thin films deposited by a RF magnetron sputtering method depend strongly on substrate temperature, bottom electrode materials, film thickness, and

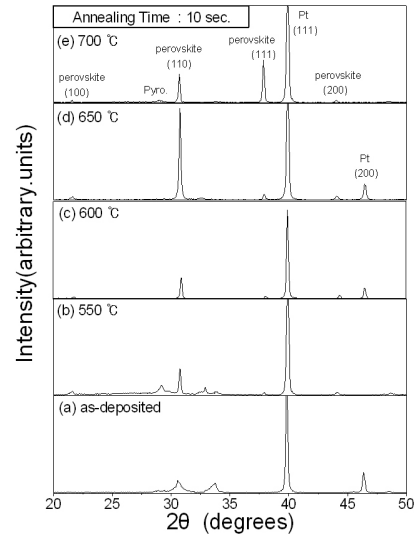


**Fig. 2.** X-ray diffraction patterns of PNZST thin films annealed at different temperatures.

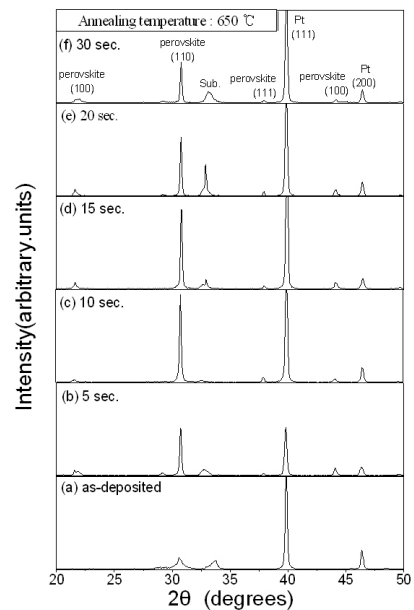


**Fig. 3.** X-ray diffraction patterns of PNZST thin films annealed at different times.

annealing conditions [11]. Figure 1 shows the X-ray diffraction curves of PNZST thin films deposited at different substrate temperatures, ranging from 350°C to 550°C. For the PNZST thin film deposited at 350°C, the dominant peak observed at  $2\theta = 40^\circ$  was a result of the (111)-oriented Pt, and (111)-oriented perovskite phase peak appeared at  $2\theta = 38.1^\circ$ . However, the pyrochlore phase peak was also observed at  $2\theta = 29^\circ$ . For the PNZST thin film deposited at 400°C, the intensity of the (111)-oriented perovskite phase peak increased. However, the intensity of pyrochlore phase peak also increased, as shown in Fig. 1(b). As the substrate temperature increased from 400°C to 450°C, the intensity of the pyrochlore phase peak decreased. When the substrate temperature increased to 500°C, the (110)-oriented perovskite peak began to appear at  $2\theta = 30.9^\circ$  and pyrochlore phase peak disappeared, as shown in Fig. 1(d). But, the intensity of the perovskite phase

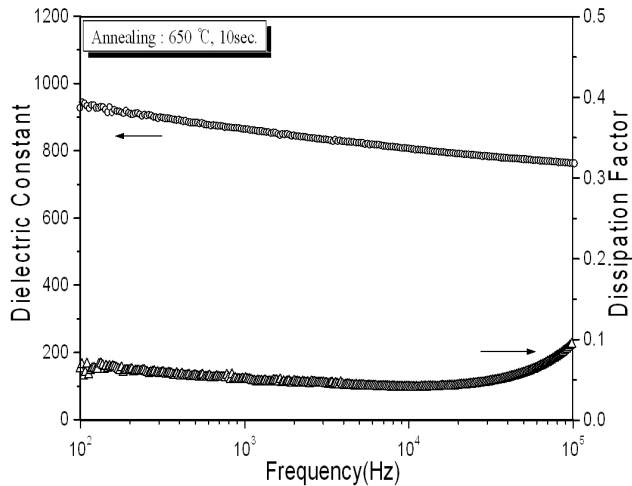


Fig. 4. Plot of the dielectric constant and dissipation factor of the PNZST capacitor.

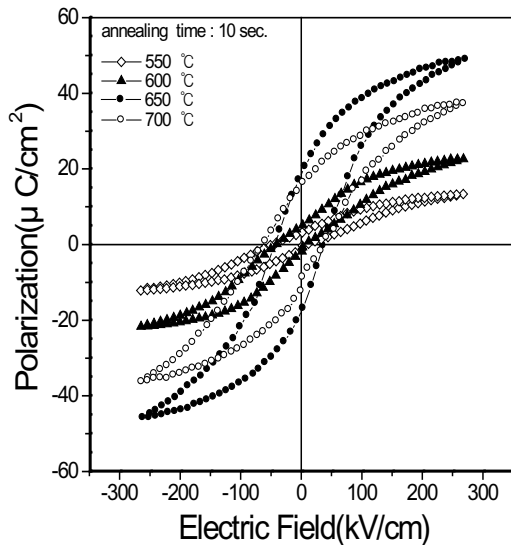


Fig. 5. P-E hysteresis loops of the PNZST capacitor.

was not high. For the PNZST thin films deposited over 500°C, the intensity of the (110)-oriented perovskite phase peak decreased, and the (111)-oriented perovskite phase peak coexisted with pyrochlore phase, as shown in Fig. 1(e). These results show that a suitable substrate temperature promotes crystallinity of the perovskite phase.

PNZST thin films were deposited at the substrate temperature of 500°C, and then annealed at different temperatures for 10 seconds in air. The X-ray diffraction curves of the PNZST are shown in Fig. 2. The (110)-oriented PNZST main perovskite peak existed in all cases, and its intensity was much stronger than any other PNZST peaks except for the Pt peak; thus indicating that the annealing process improves crystallinity of the (110)-oriented PNZST perovskite phase and depresses crystallinity of the pyrochlore phase. According to the increase of the annealing temperature, the intensity of the (110)-oriented perovskite peak increased at  $2\theta = 30.9^\circ$ , and its magnitude was the largest at 650°C, as shown in Figs. 2(b)-(d). In Fig. 2(e), when the annealing temperature increased to 700°C, the intensity of the (111)-oriented PNZST perovskite peak increased, while the other peaks had negligible

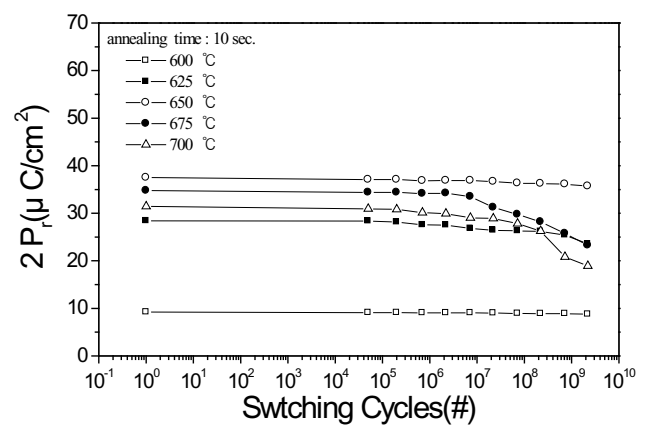


Fig. 6. Fatigue characteristics of the PNZST capacitor.

changes. This reveals that the annealing temperature has a greater and more significant effect on the crystallinity of thin films rather than the substrate temperature [12]. Perovskite-type PNZST thin films can be obtained by RF magnetron sputtering provided that the films are annealed at high temperatures. Hence, the annealing process benefits the formation of the crystalline perovskite phase. Figure 3 shows the X-ray diffraction curves of the PNZST thin films deposited at the substrate temperature of 500°C and then annealed in air at 650°C for various times. For the PNZST thin film annealed at 650°C for 10 seconds, the intensity of the (100)-oriented perovskite peak was the largest.

### 3.2 Dielectric properties

Figure 4 shows the dielectric constant and the dissipation factor of the PNZST thin films as a function of frequency. In this measurement, the PNZST thin films were deposited at the substrate temperature of 500°C, and annealed at 650°C for 10 seconds in air. The amplitude of the ramp voltage was 10 mV and the frequency ranged from 100 Hz to 100 kHz. The observed values of the dielectric constant and dissipation factor at 1 kHz were approximately 861 and 0.05, respectively. The decrease in the dielectric constant may be attributed to the effects of the interfacial polarization at the contacts and Maxwell-Wagner polarization of grain boundaries [13].

The ferroelectric properties were investigated by measuring the polarization hysteresis loop, as shown in Fig. 5. The PNZST thin films were deposited at the substrate temperature of 500°C, and annealed at different temperatures for 10 seconds in air. From Fig. 5, the remanent polarization and coercive field of the PNZST thin film annealed at 650°C were approximately 20  $\mu\text{C}/\text{cm}^2$  and 50 kV/cm, respectively. These values were superior to those obtained for sol-gel derived PNZST films [9], and exhibited a low coercive field. In our results, it is thought that a low coercive field is due to the decrease of the space charge layer inside each ferroelectric domain by doping Sn and Nb in PZT [12]. In general, the slightly lower  $P_r$  and higher  $E_c$  may be associated with the smaller grain size in thinner films. The increase in  $E_c$  with decreasing film thickness is attributed to stresses induced in the films [14], and similar effects are also observed for bulk ceramics. This effect is due to the space charge layer inside each ferroelectric domain [15].

Figure 6 shows fatigue characteristics of the PNZST capacitor. In this measurement, the amplitude of the applied bipolar pulse stress was 167 kV/cm. For the PNZST thin film deposited at 500°C and annealed at 650°C for 10 seconds in air, the reduction of  $2P_r$  after  $2.2 \times 10^9$  switching cycles is less than 10%. This result

is also observed in the sol-gel derived PZT capacitor with a LSCO bottom electrode [6], and it is thought that the PNZST thin film matches the bottom electrode in the interface.

#### 4. CONCLUSIONS

In summary,  $\text{Pb}_{0.99}[(\text{Zr}_{0.6}\text{Sn}_{0.4})_{0.9}\text{Ti}_{0.1}]_{0.98}\text{Nb}_{0.02}\text{O}_3$  ferroelectric thin films have been deposited by RF magnetron sputtering. After annealing, the thin films were completely crystallized into the perovskite phase. When the thin films were deposited at the substrate temperature of 500°C, and were annealed at 650°C for 10 seconds in air, these films exhibited good crystallinity and ferroelectric properties. Typical values for the remanent polarization and the coercive field are about 20  $\mu\text{C}/\text{cm}^2$  and 50  $\text{kV}/\text{cm}$ , respectively.

#### REFERENCES

- [1] J. F. Scott and C. A. Paz de Araujo, *Science* **246**, 1400 (1989) [DOI: 10.1126/science.246.4936.1400].
- [2] W. A. Geideman, *IEEE Trans. Ultrason. Ferroelectr. Freq. Control* **38**, 704 (1991) [DOI: 10.1109/58.108872].
- [3] S. K. Hong, *Bulletin of KIEEME*, **21**, 23 (2008).
- [4] H. J. Noh, S. P. Nam, Y. H. Lee, and S. G. Lee, *Trans. Electr. Electron. Mater.* **10**, 49 (2009).
- [5] H. M. Tsai, P. Lin, and T. Y. Tseng, *Appl. Phys. Lett.* **72**, 1787 (1998) [DOI: 10.1063/1.120571].
- [6] S. M. Yoon, E. Tokumitsu, and H. Ishiwara, *Jpn. J. Appl. Phys.* **37**, L936 (1998) [DOI: 10.1143/JJAP37.L936].
- [7] R. D. Klissurska, K. G. Brooks, I. M. Reaney, C. Pawlaczyk, M. Kosec, and N. Setter, *J. Am. Ceram. Soc.* **78**, 1513 (1995) [DOI: 10.1111/j.1151-2916.1995.tb08846.x].
- [8] J. H. Oh, J. N. Lim, S. S. Lee, and K. J. Lim, *Trans. Electr. Electron. Mater.* **10**, 169 (2009).
- [9] J. H. Jang and K. H. Yoon, *Jpn. J. Appl. Phys.* **37**, 5162 (1998) [DOI: 10.1143/JJAP37.5162].
- [10] W. C. Choi, H. H. Choi, M. K. Lee, and T. H. Kwon, *Proceedings of Fall Conference IEEK (1999 Nov., Institute of Electronics Engineers of Korea)* p. 199.
- [11] D. X. Lu, E. M. W. Wong, E. Y. B. Pun, J. S. Liu, and Z. Y. Lee, *Int. J. Electron.* **83**, 805 (1997) [DOI: 10.1080/002072197135076].
- [12] D. X. Lu, E. Y. B. Pun, E. M. W. Wong, P. S. Chung, and Z. Y. Lee, *IEEE Trans. Ultrason. Ferroelectr. Freq. Control* **44**, 675 (1997) [DOI: 10.1109/58.658328].
- [13] G. Arlt, *Ferroelectrics* **91**, 3 (1989) [DOI: 10.1080/00150198908015725].
- [14] E. S. Ramakrishnan and W. Y. Hwang, *J. Vac. Sci. Technol. A* **10**, 69 (1992) [DOI: 10.1116/1.578152].
- [15] M. Klee, R. Eusemann, R. Waser, W. Brand, and H. Van Hai, *J. Appl. Phys.* **72**, 1566 (1992) [DOI: 10.1063/1.351726].